ECCOMAS Congress 2016
VII European Congress on Computational Methods in Applied Sciences and Engineering
M. Papadrakakis, V. Papadopoulos, G. Stefanou, V. Plevris (eds.)
Crete Island, Greece, 5–10 June 2016

A COROTATIONAL FINITE ELEMENT TO MODEL BENDING VIBRATIONS OF METALLIC STRANDS

Francesco Foti[1]

[1] Politecnico di Milano, Dep. of Civil and Environmental Engineering
P.zza L. Da Vinci 32, 20133, Milano, Italy
e-mail: francesco.foti@polimi.it

Keywords: Corotational finite elements, cable dynamics, hysteretic bending, friction.

Abstract. *A new formulation to model the mechanical response of metallic strands undergoing a combination of axial load and planar bending is developed. Each wire of the strand is modeled as an elastic curved thin rod. A kinematic model is then introduced to relate the generalized strain variables of the strand to those of the wires. The stress-strain state of the wires is evaluated starting from the analysis of the internal contact conditions. Friction is modeled through the classic Amontons-Coulomb law and the elastic tangential compliance of contact patches is accounted for. A non-holonomic material constitutive law in terms of the cross sectional generalized stresses and strains of the Euler-Bernoulli beam theory is obtained and implemented within a corotational beam element explicitly conceived for nonlinear static and dynamic analyses of flexible structures. Numerical applications are presented to highlight the role of the tangential compliance mechanism on the hysteretic bending behavior of a typical steel strand.*

1 INTRODUCTION

Metallic strands can be regarded as composite elements which are made of helical wires twisted around a straight core and grouped in concentric layers. They are widespread structural members, used in many engineering applications, e.g. overhead electrical lines, tensile structures, guyed masts and towers.

When a strand is bent, wires tend to slip relatively one to each other, as a consequence of the axial force gradient generated along their length. The relative displacements are contrasted by friction forces, which are a function of the geometry of the internal structure, the material properties of the wires and the intra- and inter-layer contact pressures. If the forces which tend to activate sliding are greater than the friction ones, then a generic wire can experience relative displacements with respect to the neighbors. Interwire sliding phenomena makes the bending behavior of strands inherently non-linear and can significantly affect both the local response of the elements under cyclic loading (e.g. leading to the occurrence of fretting fatigue and wear [11, 18]) as well as the overall structural response. In fact, bending vibrations of metallic strands are characterized by an hysteretic damping mechanism, as it can be inferred from both quasi-static [17] as well as dynamic tests [21].

In the present paper, a new formulation to model the mechanical response of metallic strands undergoing a combination of axial load and planar bending is developed. Each wire of the strand is modeled as an elastic curved thin rod. A kinematic model is then introduced to relate the generalized strain variables of the strand to those of the wires. The stress-strain state of the wires is then evaluated starting from the analysis of the internal contact conditions. Friction is modeled through the classic Amontons-Coulomb law and the elastic tangential compliance of contact patches is accounted for, aiming at extending a previous authors' model taking into account the gross sliding only [3, 5, 7-9]. A non-holonomic material constitutive law in terms of the cross sectional generalized stress and strains of the Euler-Bernoulli beam theory is obtained, which can be exploited to describe cables as structural members reacting to a generic combination of axial force and bending. The sectional constitutive law is then implemented within a corotational beam element, previously developed and able to deal with large displacements and rotations and explicitly conceived for the nonlinear static and dynamic analysis of flexible structures [3, 6, 10].

The new mechanical model developed in this work is presented with reference to a simple strand made of a single layer of wires, in order to focus on the most important aspects of the proposed approach, while avoiding additional difficulties and cumbersome calculations stemming from a more complex internal geometry.

Numerical applications of the proposed cross sectional and finite element formulations are then presented for the case of a well documented steel strand, extensively studied in literature both for a combination of axial-torsional loads [4, 15, 16, 19, 20] as well as under the combined action of axial load and planar bending [9].

Within this context, systematic comparisons are carried out among the predictions of the new formulation and those of the model previously developed by the author and neglecting the interwire tangential contact compliance. The aim is to assess the effects of the tangential contact compliance on the hysteretic bending behavior of the strand. The latter, in turn, plays a key role in the modeling of the flexural vibrations of metallic strands.

2 GEOMETRY OF THE STRAND

A strand made of a single layer of six round wires, wrapped around an initially straight core wire, is considered in this work (Figure 1). The core and external wires have diameters d_0 and d_1, respectively. Each wire can be described as a curved thin rod, defined by the position of the centerline within a reference system attached to the strand centerline (axes $\{x_i\}$ (i=1, 2, 3)) as depicted in Figure 1. The centerline of the external wires is a circular helix spanned by the position vector:

$$\mathbf{x}(\theta) = \frac{R}{\tan(\alpha)}(\theta - \theta_0)\mathbf{e}_1 + R\cos(\theta)\mathbf{e}_2 + R\sin(\theta)\mathbf{e}_3 \tag{1}$$

where: $\{\mathbf{e}_i\}$ are the unit vectors of the axes $\{x_i\}$, R is the *helix radius*, i.e. the distance measured on the plane (x_2, x_3) from the centroid of the wire to that of the strand, α is the lay angle, i.e. the constant angle which the tangent vector to the helix defines with the strand centerline (axis x_1), and θ is the *swept angle*, i.e. the angle which the projection of the position vector $\mathbf{x}$ on the plane x_1=0 makes with the axis x_1 (see Figure 1(b)). The symbol θ_0 is adopted to denote the value of the swept angle at the strand cross section identified by the coordinate: x_1=0.

The external wires are assumed in contact with the core, but not among them. This condition, commonly referred to as *radial contact* condition (e.g. [1]), is typical of metallic strands.

As a consequence the helix radius in the reference (undeformed) configuration of the strand is the sum of the wire radii: R=0.5(d_0+d_1). The lay angle must be smaller than the maximum value $\alpha_{\max}$, that causes contact among the wires of a layer (see e.g. [2]).

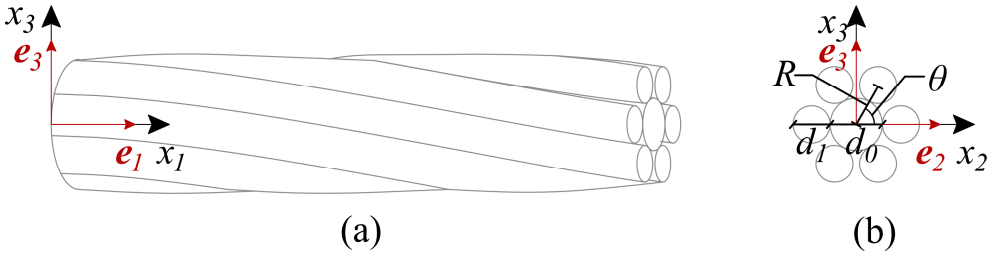

Figure 1: Geometry of the strand. (a) Side view. (b) Cross section.

3 MECHANICAL MODEL OF THE STRAND

The response of the strand to a constant axial force F_s and bending moment distribution M_s is first studied. The geometric nonlinearities, which typically affect the behavior of such slender structural elements, then, are fully considered within the framework of the corotational beam element formulation.

A “two-stage” approach is adopted in this work to tackle the axial-bending problem. As outlined e.g. in [1], the solution of the bending problem is superimposed on the initial state of stress and deformation due to the axial load. The axial force in a generic wire of the layer (tangent to the wire centerline), hence, can be expressed through the sum of a first contribution due to the axial load ($F_{w1,a}$) and a second one due to the bending of the strand ($F_{w1,b}$):

$$F_{w1} = F_{w1,a} + F_{w1,b} \tag{2}$$

3.1 Solution of the axial problem

The axial response of small-diameter metallic strands is substantially linear for a broad range of loads corresponding to typical service conditions (see e.g. the experimental results in [19] and the numerical simulations in [4, 9]). Accordingly, geometric nonlinearities due to the variation of the internal strand geometry, such as the contraction of the wire diameters (Poisson's effect) and the wire flattening (normal deformation of internal contact surfaces), can be practically neglected without significantly affecting the results.

A model for the linear coupled axial-torsional response of strands has been presented in [3, 9]. Whenever an axial load F_s is applied to the simple strand considered in the present paper, the axial elongation of the strand can be evaluated (under the assumption of zero torsional rotations of the cross sections) as:

$$\varepsilon_s = \frac{F_s}{EA_s} \tag{3}$$

where EA_s is the direct axial stiffness of the strand. By denoting as EA_0 and EA_1 the axial stiffness of the core and external wires, respectively, the strand stiffness EA_s is given by:

$$EA_s = EA_0 + 6EA_1 \cos^3(\alpha) \tag{4}$$

The axial force in the wires of the layer, then, can be expressed as:

$$F_{w1,a} = \cos^2(\alpha)\frac{EA_1}{EA_s}F_s \tag{5}$$

The axial force $F_{w1,a}$ is the same for all wires of the layer and constant along their length.

3.2 The contact model

The external wires are in contact with the core along a continuous helix (linear contact) with the same pitch of the wire centerline (see [8, 9] for more details). A system of radial (P) and tangential (T) forces per unit length of the wire centerline is first defined to model the interaction between a generic wire and the core, as shown in Figure 2. Then, the indefinite equilibrium equations of the wire in radial and tangential direction are written as:

$$\begin{cases} \dfrac{F_{w1,a} + F_{w1,b}}{\rho} - P = 0 \\ \dfrac{dF_{w1,b}}{dS} - T = 0, \ \text{ with: } \ T \le \mu P \end{cases} \tag{6a, b}$$

where ρ is the curvature radius of the wire centerline, which can be evaluated starting from equation (1) as: $\rho = R/\sin^2(\alpha)$ and μ is the friction coefficient of the contact interface.

The radial contact force P can be obtained by solving equation (6a). By neglecting the contribution $F_{w1,b}/\rho$ due to the bending of the strand, the following expression is obtained:

$$P \simeq \frac{F_{w1,a}}{\rho} \tag{7}$$

While introducing a great simplification in the analysis of the interwire contact conditions, the approximation introduced in (7) doesn't affect significantly the solution of the bending problem, as it has been shown numerically in [3] and analytically in [8] for the more general case of multi-layer metallic strands.

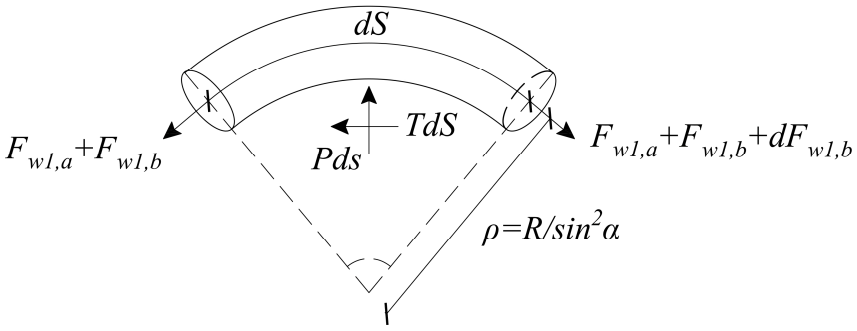

Figure 2: Equilibrium of an infinitesimal segment of the wire.

The tangential force T is related to the gradient of the wire axial force through the tangential equilibrium equation (6b). Since the term $F_{w1,a}$ stemming from the solution of the axial problem is constant along the length of the wire (see equation (5)), only the gradient of the bending contribution $F_{w1,b}$ to the total wire axial force is present in (6b).

The axial force gradient gives the wires the trend to slip with respect to the underlying core. This relative displacement is contrasted by the tangential contact force T, whose values are bounded by the Amontons-Coulomb inequality: $T \leq \mu P$. As long as $T < \mu P$, the sliding between the wire and the core is prevented (*no-sliding regime*). Relative displacements between the wire centerline (which will be denoted in the following as u_t) and the core, however, are present also in the no-sliding regime because of the tangential compliance of the contact surface. Goudreau et al. [12] studied the tangential compliance mechanism between the external wires and the core of a strand by exploiting the solution of the Hertzian contact problem for two parallel cylinders, made of the same material and pressed together. Accordingly, they introduced a non-linear relation between the relative displacement u_t and the tangential force per unit length T, herein re-stated as follows:

$$u_t = u_t^{gs}(P)\left(1-\left(1-\frac{T}{\mu P}\right)^{\frac{2}{3}}\right), \quad \text{with: } T \leq \mu P \tag{8}$$

where $u_t{}^{gs}(P)$ is the value of the relative displacement at the onset of gross sliding. The displacement $u_t{}^{gs}$ is a function of the normal contact force P. By denoting as $C_{Ti}(P)$ the initial value of the tangential compliance of the contact surface, $u_t{}^{gs}$ can be expressed as:

$$u_t^{gs} = \frac{3C_{Ti}(P)}{2\mu P} \tag{9}$$

The initial tangential compliance, in turn, depends upon the normal contact compliance $C_n(P)$ of the surface, according to the following relation, first proposed by Hobbs and Raoof [13] and later adopted also by Goudreau et al.:

$$C_{Ti}(P) = \frac{C_n(P)}{2(1-\nu)} \tag{10}$$

where ν is the Poisson coefficient of the material. A closed-form expression of the normal contact compliance $C_n(P)$ has been also derived by Goudreau et al. for the special case of ν=0.3, herein re-written, by denoting as E the Young modulus of the material, as:

$$C_n(P) = \frac{1}{E}\left(0.068505 + 1.1586 \ln\left(\sqrt{0.54945 \frac{E d_0}{P}\left(1 + \frac{d_1}{d_0}\right)}\right)\right) \tag{11}$$

A linear approximation of the model by Goudreau et al. is adopted in this work to characterize the tangential compliance between wires and core in the no-sliding regime. Based on the initial value of the tangential compliance, the following relation is introduced:

$$T \simeq \frac{1}{C_{Ti}(P)} u_t \leq \mu P \tag{12}$$

3.3 Solution of the bending problem

The nonlinear bending of multilayer strands has been studied in [3, 5, 7-9], starting from a description of the wire kinematics which accounts for the possible activation of gross-sliding phenomena, but neglects the effects of the tangential contact compliance. The aforementioned kinematic model will be augmented to account for the tangential compliance with the core wire.

By recalling equation (1) and assuming all wires as linearly elastic, the axial strain of a generic wire, ε_{w1}, can be expressed as the sum of the strain due to the axial load and to the bending, i.e.:

$$\varepsilon_{w1} = \frac{F_{w1}}{EA_1} = \frac{F_{w1,a}}{EA_1} + \frac{F_{w1,b}}{EA_1} = \varepsilon_{w1,a} + \varepsilon_{w1,b} \tag{13}$$

Two limit kinematic hypothesis can be introduced to evaluate $\varepsilon_{w1,b}$, which will be referred in the following as: *full-stick* and *full-slip* assumption. In the first case the tangential force T, due to the friction between the wire and the core, is assumed to be large enough to prevent the gross-sliding and the effect of the tangential compliance is neglected. As a consequence, the wire behaves as a part of an ideal planar cross section and the term $\varepsilon_{w1,b}$ can be simply evaluated according to the well-known Euler-Bernoulli kinematic model:

$$\varepsilon_{w1,b}^{full-stick} = \cos^2(\alpha) R \sin(\theta) \chi_s \tag{14}$$

where χ_s is the bending curvature with respect to the axis x_2 (see Figure 1).

In the second case, instead, the wire is free to slide with respect to the core and can be considered as individually bent. Under the full-slip assumption, hence, the term $\varepsilon_{w1,b}$ is identically equal to zero. By neglecting the tangential compliance, hence, the following incremental alternatives can be introduced to account for the possible transition between the no-sliding and the gross-sliding regime:

$$\dot{\varepsilon}_{w1,b} = \begin{cases} \dot{\varepsilon}_{w1,b}^{no-sliding} = \dot{\varepsilon}_{w1,b}^{full-stick} \\ \dot{\varepsilon}_{w1,b}^{gross-sliding} = 0 \end{cases} \tag{15a, b}$$

where a dot is adopted to denote the derivative with respect to a time variable t.

Equation (15a) can be modified in order to account for the effect of the tangential compliance between the external wires and the core, based on the solution of the bending problem in no-sliding regime which will be detailed in the following.

By recalling the definition of the relative displacement u_t introduced in Section 3.2, the term $\varepsilon_{w1,b}$ can be evaluated as:

$$\varepsilon_{w1,b}^{no-sliding} = \varepsilon_{w1,b}^{full-stick} + \frac{du_t}{dS} \tag{16}$$

By observing that $\sin(\alpha)\mathrm{d}S = R\mathrm{d}\theta$ (see e.g. [8]), from equations (6b), (12), (13) and (16) it's easy to derive the following equation for the axial force $F_{w1,b}$ in the *no-sliding* regime:

$$\frac{d^2 F_{w1,b}^{no-sliding}(\theta)}{d\theta^2} - \frac{R^2}{C_{Ti} EA_1 \sin^2(\alpha)} F_{w1,b}^{no-sliding}(\theta) = -\frac{R^3 \cos^2(\alpha)\chi_s}{C_{Ti}\sin^2(\alpha)}\sin(\theta) \tag{17}$$

The equation above can be easily solved under the assumption of constant curvature of the strand. The following expression is obtained:

$$F_{w1,b}^{no-sliding}(\theta) = \frac{\cos^2(\alpha) R\, EA_1\, \chi_s}{1 + \dfrac{C_{Ti}(P) EA_1 \sin^2(\alpha)}{R^2}}\sin(\theta) \tag{18}$$

Once the function $F_{w1,b}^{no-sliding}(\theta)$ is known, the corresponding axial strain can be evaluated and used in (15, a).

A numerical strategy to evaluate the wire axial force $F_{w1,b}(\theta)$, accounting for the possible transition between *no-sliding* and *gross-sliding* regime has been developed by the author in [3, 5, 7-9] and is adopted also in this work. The numerical procedure is based on a classic *Return-Map algorithm*, based on a "*no-sliding* prediction" and a "*gross-sliding* correction" (according to the alternative kinematic equations previously discussed). The Return-Map algorithm delivers the value of the gradient of the wire axial force which satisfies equation (16b), over a discrete set of control points defined along the pitch of the wire. Then, the wire axial force is obtained through numerical integration along the wire length.

Finally, starting from the knowledge of the wire axial force in all the wires of the layer the cross sectional moment of the strand can be evaluated, through simple equilibrium considerations, as:

$$M_s = M_s^{ind} + M_s^{add} = EI_{\min}\chi_s + M_s^{add} \tag{20}$$

The first term, M_s^{ind}, in (20) is linear and stems from the individual bending of the wires. It can be simply calculated as the product of the strand curvature and the minimum bending stiffness of the strand $EI_{\min}$. The latter can be evaluated by modeling the strand as a bundle of elastic curved thin rods, individually bent. The following expression can be obtained from [8]:

$$EI_{\min} = EI_0 + 6\cos^3(\alpha) EI_1 \tag{21}$$

The second term in (20), instead, accounts for the additional moment due to the bending contribution $F_{w1,b}(\theta)$ to the total axial force of the wires and can be evaluated (see e.g. [8]) as:

$$M_s^{add} = \sum_{i=1}^{6} R\cos(\alpha) F_{w1,b}(\theta_i)\sin(\theta_i) \tag{22}$$

3.4 The corotational beam element

The equations (3) and (20) fully define the relation between generalized stress and strain variables of the strand cross section, herein regarded as a plane Euler-Bernoulli beam. The proposed constitutive equations have been implemented within a corotational beam element

previously developed [3, 6, 10] to study the static and dynamic response of flexible structures taking into account geometrical and material nonlinearities.

4 NUMERICAL APPLICATION

The proposed strand mechanical model and beam finite element formulation are applied in this section to investigate the bending response of a strand made of steel wires, already studied in [9]. The geometric and material properties of the element are listed in Table 1.

d_0 (mm)	d_1 (mm)	α (deg)	E (GPa)	ν (-)
3.94	3.73	11.8	188	0.3

Table 1: Geometric and material parameters from [15].

The wire axial force in the no-sliding regime is shown in Figure 3 in terms of the amplification factor q_F of the force equivalent to $F_{w1,b}^{no-sliding}$ but obtained (under the full-stick assumption) by neglecting the tangential compliance. The factor q_F is plotted in Figure 3 as a function of the non-dimensional axial load parameter η, defined as the ratio between the axial load F_s and the Rated Tensile Strength of the element (here 137 kN – see [19]). From Figure 3, it can be observed that the inclusion of the tangential compliance mechanism in the strand mechanical model leads to a reduction of 10% of the maximum value which can be attained by the wire axial force $F_{w1,b}$ in the no-sliding regime with respect to the full-stick solution. The value of q_F depends on the non-dimensional loading parameter η. By increasing the axial load, indeed, the tangential compliance is reduced, as predicted by equations (10) and (11). As a consequence the axial force $F_{w1,b}$ tends toward the full-stick solution $F_{w1,b}^{full-stick}$ for increasing values of axial load. However, it's worth noting that the ratio q_F: (a) doesn't reach the unit value, even for very large values of the axial load, close to the RTS of the strand (for which, however, the assumption of linearly elastic material adopted in the proposed formulation ceases to be valid), and (b) is only slightly dependent on the axial load for the particular strand under consideration (variations of q_F are in the order of 3% for axial loads ranging from zero to the RTS value).

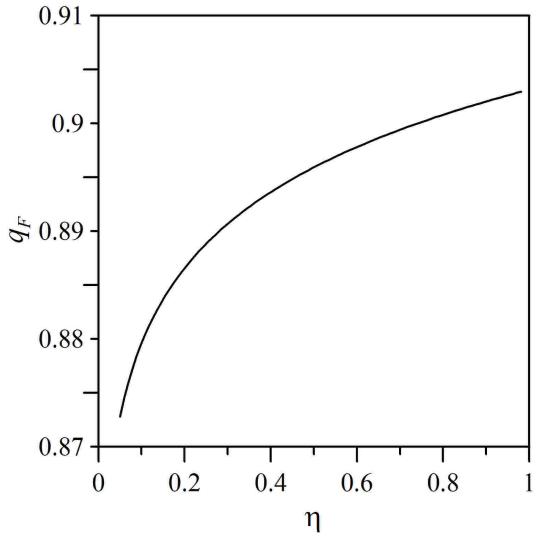

Figure 3: Ratio q_F vs. the non-dimensional axial load η.

Figure 4 shows a comparison among the moment-curvature diagrams of the strand cross section obtained with the proposed formulation, accounting for the tangential compliance of the internal contact surfaces, and those obtained by considering a full-stick initial behavior of the wires. Results are plotted for different values of the axial load parameter η in the range 0.1-0.25 (Figure 4(a)) and for different values of the friction coefficient μ in the range 0.3-0.7 (Figure 4(b)), in order to cover the interval of values typically considered in literature (e.g.: [8, 9, 14, 17]).

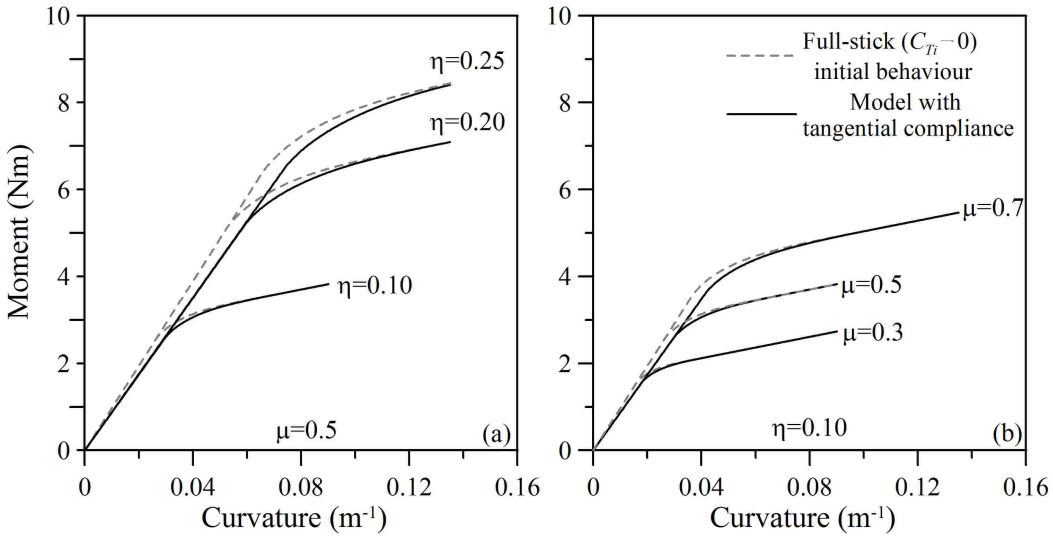

Figure 4: Moment-curvature diagrams. (a) Variation of the non-dimensional axial load η. (b) Variation of the friction coefficient μ.

The moment-curvature diagrams obtained with or without accounting for the tangential compliance mechanism are very similar, for the special strand considered in this work. In particular, the two models exhibit a similar dependency on the axial loading parameter η and on the friction coefficient μ. These parameters strongly influence the hysteretic bending behavior of metallic strands, as it has been extensively discussed e.g. in [8, 9]. The major effect of the tangential compliance between the core and the external wires is recognized in a reduction of about 10% of the value of the initial bending stiffness (i.e. the maximum bending stiffness of the strand section: $EI_{\max}$) of the cross section.

A typical experimental test setup for the characterization of the hysteretic bending behavior of metallic strands has been numerically simulated, in order to investigate the effect of the tangential contact compliance on the overall behavior of a strand specimen. A schematic representation of the numerical test setup is reported in Figure 5. The specimen is first loaded in the axial direction and then subjected to a transverse quasi-static load F. A mesh of 32 equally spaced corotational beam finite elements is adopted to represent the strand. Mesh refinements have been also considered in preliminary calculations to check the accuracy of the numerical model. A friction coefficient equal to 0.5 has been assumed in all the analyses.

Figures 6(a) and 6(b) show the load-displacement curves of the strand for a monotonically increasing vertical load and two different values of axial load, namely: η=0.1 (Figure 6(a)) and η=0.2 (Figure 6(b)). The load-displacement curves obtained both with and without considering the tangential compliance are plotted in Figures 6(a) and 6(b), together with the reference elastic solutions (plotted with red dashed lines) calculated under the full-stick ($EI_{\max}^{full-stick}$) and the full-slip ($EI_{\min}$) kinematic assumptions. The main effect of the tangential

compliance mechanism can be recognized in a reduction of the initial stiffness of the load-displacement curves, of about 10% for the slacker strand (η=0.1) and 1% in the other case (η=0.2). The influence of the tangential compliance mechanism on the specimen behavior, hence, is similar to the influence on the cross sectional response. However, a more pronounced dependency on the value of the axial load is observed for the overall specimen response than for the individual cross section behavior.

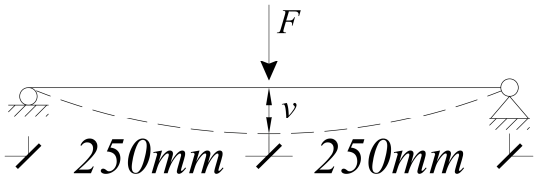

Figure 5: Structural scheme of the setup.

Additional numerical tests under cyclic vertical loading have shown that, for the special strand considered in this paper, the tangential compliance mechanism affects very slightly both the shape as well as the area of the hysteresis loops.

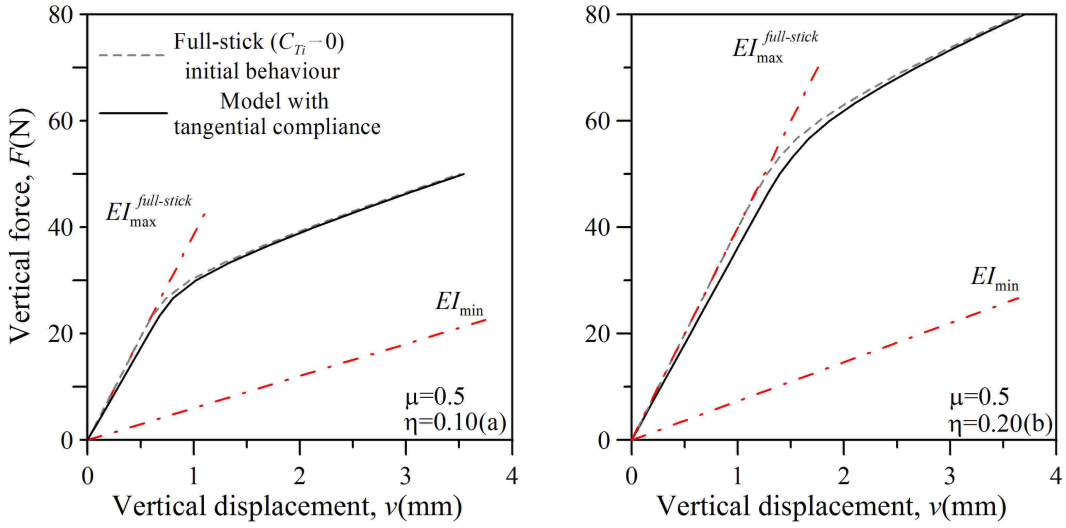

Figure 6: Bending behavior of the strand. (a) Monotonic loading. Load vs. displacement curve, μ=0.5 and η=0.10. (b) Monotonic loading. Load vs. displacement curve, μ=0.5 and η=0.20.

5 CONCLUSIONS

A new mechanical model to study the mechanical response of metallic cables undergoing a combination of axial load and planar bending has been developed for a single-layer strand. The proposed formulation is based on a detailed analysis of the internal contact conditions between the external wires and the core of the strand. Friction is modeled through the classic Amontons-Coulomb law and the elastic tangential compliance of contact patches is accounted for, aiming at extending a previous authors' model taking into account the gross sliding only. A nonlinear and non-holonomic relation between the sectional generalized stress and strains of the Euler-Bernoulli beam theory is formulated and implemented in a corotational beam element suitable for nonlinear static and dynamic analyses of flexible structures.

The proposed strand mechanical model and finite element formulation have been applied to characterize the hysteretic bending behavior of a common structural steel strand. Numerical

analyses have been carried out to show the influence of the tangential contact compliance mechanism between the external wires and the core, both on the cross sectional behavior as well as on the overall response of a strand specimen tested on a typical experimental test rig.

For the particular strand considered in this work, it is found that the tangential contact compliance mainly influence the initial bending stiffness of the strand, while it has only a small effect on the shape of the cross sectional moment-curvature diagrams and on the overall hysteretic behavior. Ongoing research is devoted to the extension of the proposed formulation to other strand geometries, including the case of multi-layer elements.

REFERENCES

[1] A. Cardou, C. Jolicoeur, Mechanical models of helical strands, *Applied Mechanics Reviews* (ASME), **50**, 1-14, 1997.

[2] G.A. Costello, *Theory of wire ropes*, Springer-Verlag, New York (USA), 1990.

[3] F. Foti, *A corotational beam element and a refined mechanical model for the nonlinear dynamic analysis of cables*, Doctoral Dissertation, Politecnico di Milano, Milan (Italy), 2013.

[4] F. Foti, A. de Luca di Roseto, Analytical and Finite Element modelling of the elastic-plastic behaviour of metallic strands under axial-torsional loads, Submitted to: *International Journal of Mechanical Sciences*, 2016.

[5] F. Foti, L. Martinelli, A model for the cyclic biaxial bending of stranded ropes (in Italian), *XX Congresso AIMETA 2011*, Bologna (Italy), (ISBN:9788890634017) 2011.

[6] F. Foti, L. Martinelli, Dynamics of co-rotational beam elements – some aspects on the kinetic energy and the integration of the equations of motion. J. Eberhardsteiner et.al. eds. *Proceedings of the 6th European Congress on Computational Methods in Applied Sciences and Engineering (ECCOMAS)*, Vienna (Austria), (ISBN:978-3-9502481-9-7) 2012.

[7] F. Foti, L. Martinelli, A corotational beam element to model the hysteretic bending behavior of metallic wire ropes, *The 4th Canadian Conference on Nonlinear Solid Mechanics (CanCNSM 2013)*, Montreal (Canada), 2013.

[8] F. Foti, L. Martinelli, An analytical approach to model the hysteretic bending behavior of spiral strands, *Applied Mathematical Modelling*. in press (http: //dx.doi.org/ 10.1016/j.apm.2016.01.063), 2016.

[9] F. Foti, L. Martinelli, Mechanical modeling of metallic strands subjected to tension, torsion and bending, Submitted to: *International Journal of Solids and Structures*, 2016.

[10] F. Foti, L. Martinelli, F. Perotti, Numerical integration of the equations of motion of structural systems undergoing large 3D rotations: dynamics of corotational slender beam elements, *Meccanica*, **50**, 751-765, 2015.

[11] M Giglio, A Manes, Bending fatigue on a metallic wire rope for aircraft rescue hoist, *Engineering Failure Analysis*, **10**, 223-235, 2003.

[12] S Goudreau, F Charette, C Hardy, L Cloutier, Bending Energy Dissipation of Simplified Single-Layer Stranded Cable, Journal of Engineering Mechanics (ASCE), **124**, 811-817, 1998.

[13] R.E. Hobbs, M. Raoof, Interwire slippage and fatigue prediction in stranded cables for TLP tethers. C. Chryssostomiolis and J.J. Connor eds. *Proceedings of the 3rd International Conference on Behaviour of offshore structures*, Vol. 2, Hemisphere Publishing/McGraw-Hill, New York (USA), 77-99, 1982.

[14] K.J. Hong, A. Der Kiureghian, J.L. Sackman, Bending behavior of helically wrapped cables, Journal of Engineering Mechanics (ASCE), **131**, 500-511, 2005.

[15] W.G. Jiang, M.S. Yao, J.M. Walton, A concise finite element model for simple straight wire rope strand, *International Journal of Mechanical Sciences*, 41, 143-161, 1999.

[16] R. Judge, Z. Yang, S.W. Jones, G. Beattie, Full 3D finite element modelling of spiral strand cables, *Construction and Building Materials*, **35**, 452-459, 2012.

[17] K.O. Papailiou, On the bending stiffness of transmission line conductors, *IEEE Transaction on Power Delivery*, **12**, 1576-1588, 1997.

[18] M.A. Urchegui, W. Tato, X. Gómez, Wear Evolution in a Stranded Rope Subjected to Cyclic Bending, *Journal of Materials Engineering and Performance*, **17**, 550-560, 2008.

[19] W.S. Utting, N. Jones, The response wire rope strands to axial tensile loads – Part I. Experimental results and theoretical predictions, *International Journal of Mechanical Sciences*, **29**, 605-619, 1987.

[20] W.S. Utting, N. Jones, Response of wire rope strands to axial tensile loads. Part II: comparisons of experimental results and theoretical predictions, *International Journal of Mechanical Sciences*, **29**, 621-636, 1987.

[21] Z.H. Zhu, S.A. Meguid, Nonlinear FE-based investigation of flexural damping of slacking wire cables, *International Journal of Solids and Structures*, **44**, 5122–5132, 2007.